Diyala Journal of Engineering Sciences

Journal homepage: https://djes.info/index.php/djes

ISSN: 1999-8716 (Print); 2616-6909 (Online)

Analytical and Experimental Analysis of the Shape Recovery Behavior of Continuous Fiber Reinforced Shape Memory Polymer

Wessam Saadoun Al Azzawi *

Department of Materials Engineering, University of Diyala, 32001 Diyala, Iraq

ARTICLE INFO

Article history:
Received July 5, 2023
Revised December 3, 2023
Accepted December 6, 2023
Available online December 15, 2023

Keywords:

Analytical analysis
SMP composites
Shape recovery
Thermomechanical analysis

ABSTRACT

Shape memory polymer (SMP) signify a new category of responsive polymers characterized by their capability to undergo significant shape changes and then revert to their initial shape when exposed to specific stimuli. They are known by their low mechanical properties; however, when integrated into fiber-reinforced composites a considerable characteristics enhancement is achieved. Modeling the thermomechanical behaviour of these materials is crucial task to understand their shape fixity and recovery. However, the available models in the literature are sophisticated and not easy to implement. In this study a simplified mathematical model is presented, based on the stimulus temperature-time relation, to determine the shape recovery action in a woven glass fiber (GF) reinforced styrene based SMP. The model is validated using experimental investigations done with DMA Q800 analyser and a specially designed bending recovery tool where a slight deviation of (8%-16%) was achieved. The model findings showed significant reduction in recovery time of 25% and 41% when the fiber content increased from 20% to 25% and 30%, respectively. This makes the proposed model a valuable tool for engineers to assess the shape memory behavior. Experimental findings indicated that fiber reinforcement led to a significant enhancement in thermomechanical properties represented by 5oC increase in glass transition temperature and five orders of increase in storage modulus. Also, a remarkable improvement in shape recovery rate of up to 80% is obtained, however there is a slight reduction of (8% - 16%) in the shape fixity property.

1. Introduction

SMPs have the ability to retain a temporary shape indefinitely after being deformed above the glass transition temperature (Tg) and subsequently cooled. this critical temperature. However, when they are heated above Tg again they regain around 100% of the initial shape [1, 2]. SMPs offer several key benefits over the shape memory alloys, including exceptional deformability, good manufacturability, and remarkable ability to recover original shape [3-5]. However, the relatively lower modulus and strength are inherent limitations of SMP, which have led to more interest in shape memory alloys [6]. Though, incorporating the SMPs into a fiber reinforcement has produced shape memory composites (SMPCs) where a fascinating improvement in mechanical and shape recovery behavior are achieved [7]. Fejős, et al. [8] conducted a shape memory characteristics comparison between pure SMP and SMPCs with glass fiber reinforcement. The results depicted an important development in recovery stress compared to neat SMP, which rose from 0.4 to 42 MPa. However; this study did not observe reinforcement impact on the recovery ratio. Both types of materials demonstrated complete shape recovery. The

* Corresponding author.
E-mail address: wisamazawi@yahoo.com
DOI: 10.24237/djes.2023.160404

impact of carbon fiber reinforcement was examined by [9]. The study introduced a woven fabric SMPC, and the results revealed a substantial development in recovery ratio and rate. [10] examined the mechanical properties enhancement due reinforcement using different materials. An improvement in toughness, strength, and modulus was reported while relatively no change in recovery rate was observed. [11] explored the shape recovery behavior of SMP reinforced carbon fibres. The research aimed to demonstrate the suitability of employing SMPC in applications like hinge in deploying structure. The study reported an enhancement in SMPC's storage modulus, along with 90% achievement in the recovery ratio.

Many studies were presented recently for modelling the SMPCs' thermomechanical cycle including the shape programming, free-, and constrained-shape recovery. Most of these studies adopt numerical methods to simulate the complicated behavior of these materials. Al Azzawi, et al. [7] introduced a numerical technique to SMPCs using the commercial ABAQUS software. The model incorporates consideration of the complicated time-dependent viscoelastic properties of the material which required sophisticated laboratory characterizations. Another study by Li, et al. [12] introduced a novel approach by treating the SMPC as composite laminates, the reinforcement fibres were represented as periodic ellipsoidal inclusions distributed within the matrix. The study employed microscopic mechanical model along with high-fidelity generalized method and introduced them into the classical lamination theory. The model is intriguing, but it requires skilled experts to carry out the computational process, which in turn calls for a high-performance processor. More recently, [13-17] proposed different constitutive models and implemented them into the commercial ABAQUS/Standard finite element software package. However, the implementation these models into the ABAQUS software is not a simple and direct forward process, it necessitates the use of UMAT user defined subroutines to introduce the material properties to the software.

While the aforementioned researches made significant assistances in modelling the SMPCs, additional studies are required to provide easier and more precise models to describe the material's thermomechanical behavior. In this paper, the author based on the stimulus temperature-time relationship to formulate a simplified and easy to implement analytical model to predict the shape recovery performance of neat styrene-passed SMP and its glass fiber SMPC. The model is based in the material glassy phase-temperature transition relation and the heating rate during the recovery process [3].

2. Materials and methods

2.1. Samples preparation

Styrene based shape memory polymer (SMP) was employed to create four distinct samples. These samples included pure SMP and three SMPCs with varying fibre fractions, all produced using woven glass fibres. Teflon coated glass surface was used to hand layup three SMPC sheets, as shown in Figure 1, with fiber weight fraction of 20%, 25%, and 30%. The fabricated sheets were cured at 75^{o}C for 24 hours in a temperature-controlled oven. Then, the specimens were cut into two sets of rectangular samples. The first set was designated for dynamic mechanical analysis and measured 35×14×1.5 mm^3 in size, while the second set was allocated for assessing shape recovery and had dimensions of 150×20×2 mm^3.

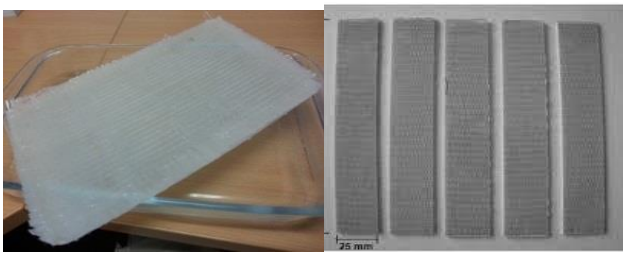

Figure 1. Glass fibre SMPC sheet fabricated using the hand layup technique

2.2 Material characterization

2.2.1 Thermomechanical analysis

Thermomechanical analysis was done to determine storage modulus of the samples and to identify glass transition temperature (T_g). For that purpose, a DMA Q800 Dynamic Mechanical Analyzer (Figure 2) was used, in dual cantilever bending arrangement, to perform scan over a temperature span of 30°C to 115°C. The process was done using frequency and temperature ramp of 1.0Hz and 10° C/min, respectively.

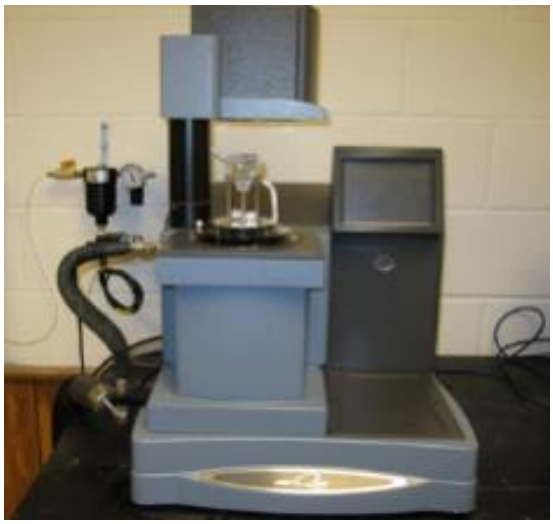

Figure 2. a DMA Q800 Dynamic Mechanical Analyzer

2.2.2 Shape recovery

Error! Reference source not found. shows a specially designed tool to test the SMPC specimens' shape fixity and recovery. Electrical oven was used a temperature chamber to provide controlled temperature environment during the shape programming and shape recovery tests. A thermocouple was affixed near the specimen to ensure precise monitoring of the specimen's temperature.

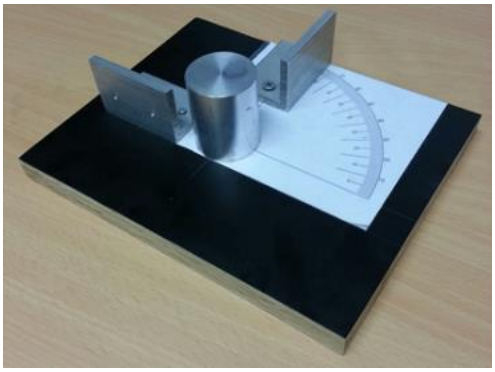

Figure 3. Specially designed tool to measure the shape recovery behavior and the shape fixity ratio

The test was performed in 4 sequential steps; firstly, the specimen was heated up to T_g and kept 5 minutes to ensure an even temperature distribution. Subsequently, it was bent to 45° angle around a cylinder with a 40 mm diameter. Subsequently, the temperature is reduced to room temperature while the bending angle is kept unchanged using a mechanical constrainer. When the specimen temperature reaches the room temperature the constrainer is removed, the storage angle is measured, and the storage ratio is calculated using flowing equation

$$R_f = \frac{\varepsilon_u}{\varepsilon_m} 100\% \quad (1)$$

Here ε_u is fixity angle, ε_m is bending angle, and R_f is the fixity ratio.

In the final step, the specimens were reentered into the temperature chamber where they were heated to T_g while the recovery process was observed using a camera as shown in **Error! Reference source not found.**.

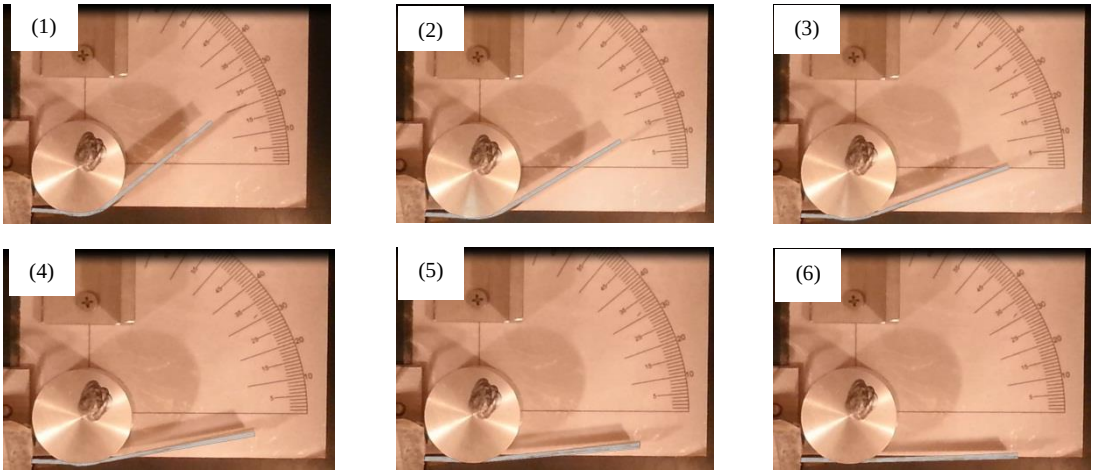

Figure 4. Bended sample shape recovery stages recorded by video camera inside the temperature chamber

3. Analyticl analysis of shape recovery

Error! Reference source not found. depicts a simplified 3-D model of a shape memory polymer. Throughout the thermomechanical cycle, at any given temperature, the polymer is considered to be a combination of two distinct phases: active phase (denoted by light region) and frozen phase (represented by dark region). As per the model introduced by [18], the shape memory characteristics can be understood by monitoring the alteration in the ratio of these two phases.

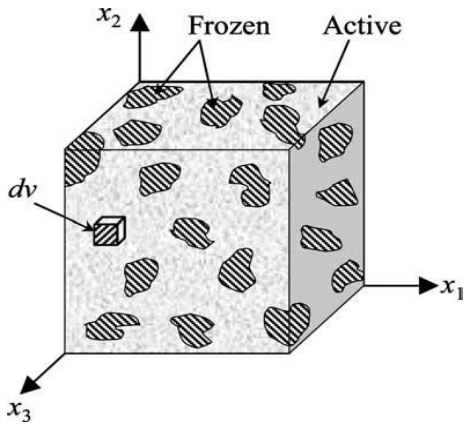

Figure 5. Schematic diagram of the micromechanics foundation of the 3-D SMP constitutive model

During cooling, frozen phase is gradually generates, and the frozen and active phase fractions are defined as:

$$\phi_a = \frac{V_{act}}{V}, \quad \phi_f = \frac{V_{frz}}{V},$$
$$\phi_a + \phi_f = 1 \qquad (2)$$

where, V, V_{act} and V_{frz} represent the overall polymer volume, volumes of the active phase and frozen phase, respectively. ϕ_a and ϕ_f are temperature dependent variables which denote the active and frozen phases fractions in the polymer.

The model suggests that when the heating rate is constant and the strain rate is slow, V_{frz} and ϕ_f are only temperature dependent [19].

$$\phi_f = \phi_f(T), \quad V_{frz} = V_{frz}(T) \qquad (3)$$

At high temperature, above T_g, deformation produced by external load can be frozen and stored inside the material when unloading at low temperature (below T_g), therefore ϕ_f has assumed to captures the storage strain in terms of temperature [18]. Also, it has assumed that the material strain is equal to the corresponding strains in active and frozen phases [19].

$$\varepsilon = \phi_f \varepsilon_f + (1 - \phi_f)\varepsilon_a \quad (4)$$

where, ε, ε_f and ε_a are the total strain, strains in the frozen and active phase, respectively. Below glass transition temperature, SMP has high modulus due to the crystalline polymer in the frozen phase, however above the transition temperature the modulus degrades significantly because of the rubbery phase. Hence, ϕ_f has derived by fitting the storage modulus-temperature curve divided by the storage modulus of the glassy phase **Error! Reference source not found.**.

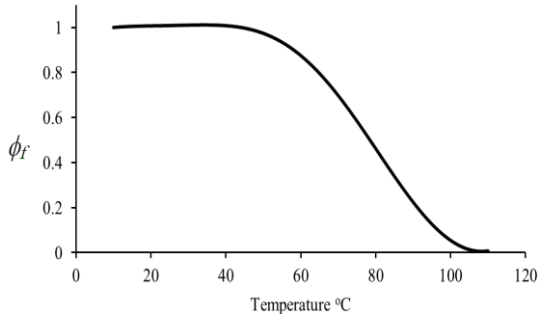

Figure 6. Relationship between temperature and the ratio of the frozen fraction

The SMPC total strain during the thermomechanical cycle is divided into two elements: mechanical and thermal, as outlined below.

$$\varepsilon = \varepsilon_m + \varepsilon_T \quad (5)$$

where, ε, ε_m, and ε_T represent the overall, mechanical, and thermal strains, respectively. Under the assumption of small strains, the SMPC employs the mixture rule, dividing the strain to matrix, fibre, and thermal strains [20].

$$\varepsilon = (1-\phi_f)\,(\varphi_r\varepsilon_r+\varphi_g\varepsilon_g+\varepsilon_s) + \phi_f\varepsilon_f + \varepsilon_T \quad (6)$$

In this context, ε_r and ε_g represent the elastic strains in the rubbery and glassy phases. ε_s represents stored and released strain during the thermomechanical cycle. Additionally, ε_f denotes the fibre's elastic strain. ε_T is defined by [21] as:

$$\varepsilon_T = \left(1 - \phi_f\right)\varepsilon_T^m + \phi_f\varepsilon_T^f \quad (7)$$

The superscript *m* and *f* indicate matrix and fibers, respectively.

Since the matrix is suggested to be composite of two phases, thermal strain is determined by adding the thermal strain of the two phases, as follows:

$$\varepsilon_T^m = \int_{T_o}^{T}\left[\left(1 - \varphi_g(T)\right)\alpha_r + \varphi_g(T)\alpha_g\right]dT \quad (8)$$

In this equation, α_r and α_g denote the coefficients of thermal expansion in rubbery and glassy phases, respectively. T and T_o are the heating process final and initial temperatures.

Based on equations (2) and (3), it can be deduced that the recovery strain is entirely governed by thermal factors [22]. In the recovery process, the material undergoes a heating procedure, during which the temperature gradually rises over time.

$$T = T(t) \quad (9)$$

Through fitting the time evolution of the heating process, a relationship between temperature and heating time has been established. This relationship can then be employed to ascertain the glassy phase volume vs time. Consequently, the recovery strain-time relationship is computed based on Equation (4).

4. Results and discussion

4.1Properties characterization

The shape recovery characteristics of both pure SMP and glass fiber-reinforced SMPCs have been examined. The introduction of glass fiber reinforcement was suggested to enhance the mechanical properties and shape memory performance of the SMP specimens.

Error! Reference source not found. depicts the loss modulus of the neat SMP and the SMPCs samples as a function of temperature. The results show mariginal increase in T_g of the investigated samples due to the inclusion of the fibre. T_g of the pure SMP, 20% SMPC, 25% SMPC, and 30% SMPC samples were determined at the peak of the loss modulus curve and measured as 63°C, 64°C, 65°C, and 68.5°C, respectively. This observation is attributed to the thermal capacity and low thermal conductivity of the glass fibre which delays the heating and softening onset of

the matrix, the same phenomenon was reported by [11].

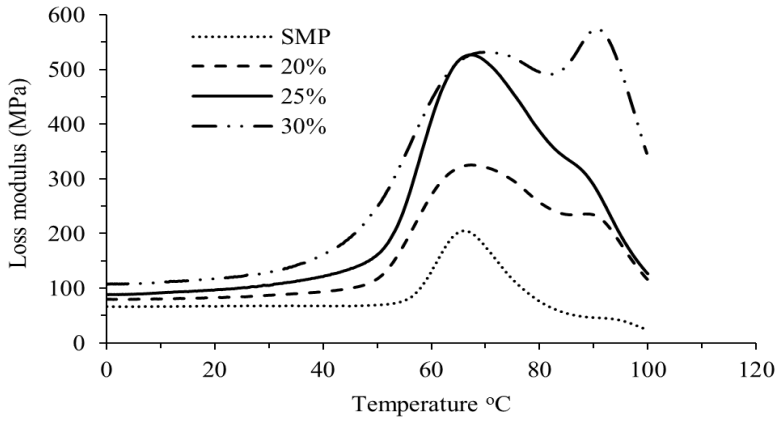

Figure 7. Loss modulus-temperature relationships of the SMP and SMPC samples

To assess the impact of fibre inclusions on the mechanical properties of the samples, the storage modulus of each sample is measured at its respective T_g using the dynamic mechanical analyser. **Error! Reference source not found.** shows significant improvement in samples' storage modulus due to the reinforcement with glass fibre which could be due to the higher stiffness of the fiber.

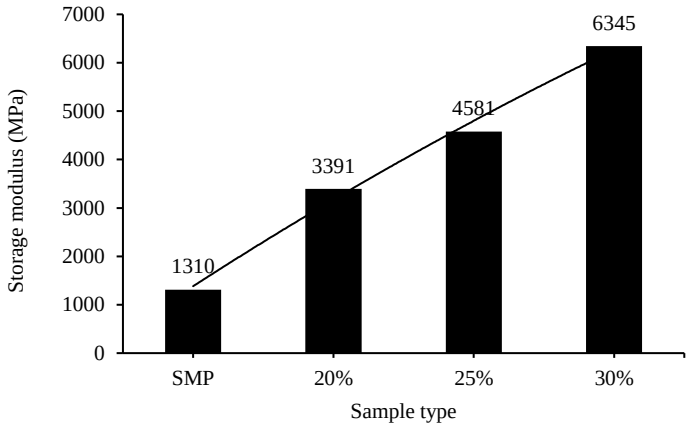

Figure 8. Storage modulus measured at the respective Tg of each sample

44.2 Shape memory characterization

The primary role of shape memory polymers lies in their capacity to establish and maintain a temporary shape, and later recall and restore the original permanent shape when prompted by heat. Therefore, when fibres are incorporated to enhance mechanical properties, it becomes crucial to examine how this reinforcement might influence the material's shape memory behaviours.

2.2.1 Shape fixity

Shape fixity serves as a measure of the SMPs' capability to retain temporary shape at the conclusion of the first stage of the thermomechanical cycle where temporary shape is programmed. In the current investigation, bending angle of the samples was utilized as a parameter to assess the material's shape fixity performance. **Error! Reference source not found.** illustrates the shape fixity ratio of the examined samples, calculated using Equation (1). The outcomes indicate a decline in the material's ability to retain its shape due to the reinforcement which is attributed to the spring

back effect of the stiffer fiber. Even with high fiber content the ratio is practically significant especially when considering the significant enhancement in thermomechanical properties associated with the reinforcement [19].

4.2.2 Shape recovery

Error! Reference source not found. (a) and (b) show experimental test findings of the shape recovery stage. The results reveal a substantial decrease in the shape recovery time due to the incorporation of fibre, affirming the beneficial impact of the reinforcement on the material's recovery behavior.

Error! Reference source not found. (b) confirms that fibre reinforcement has played major rule in reducing the recovery time. The results show that recovery time of the 20%, 25% and 30% SMPC samples is reduced by 70%, 75% and 80%, respectively, compared to the neat SMP. This is justified by the improved stiffness of the SMPC that leads to a quicker shape recovery [23].

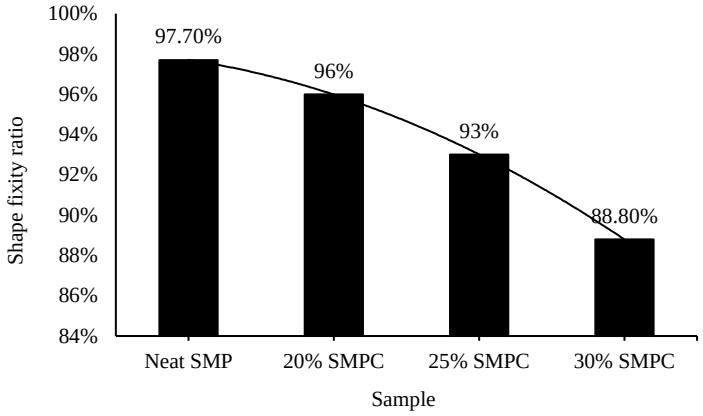

Figure 9. Shape fixity variation with glass fibre reinforcement

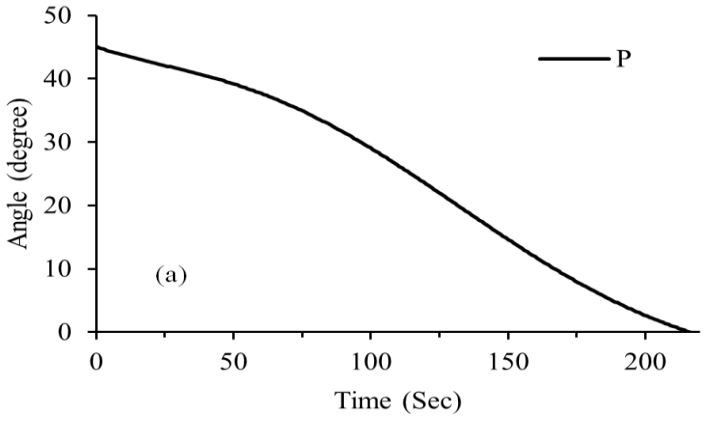

a)

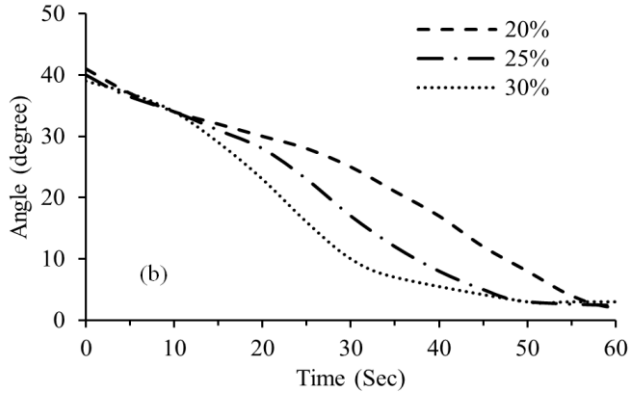

b)

Figure 10. Bending angle recovery vs time of (a) the SMP sample, and (b) different SMPCs

Error! Reference source not found. (a, b and c) illustrates the proposed analytical results for the 20%, 25% and 30% SMPCs respectively. Insipte of the simplicity of the propsed model, it shows a good ability to predict the shape recovery-time behaviour of different fibre fraction SMPCs. Though, some mismatch can be rcognised which could be attributed to potential errors in monitoring the heating process, as the used thermal chamber doesn't have the facility to provide accurate time-temperature data.

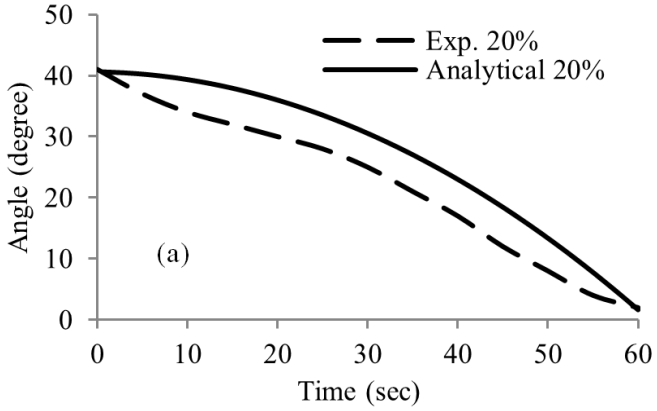

a)

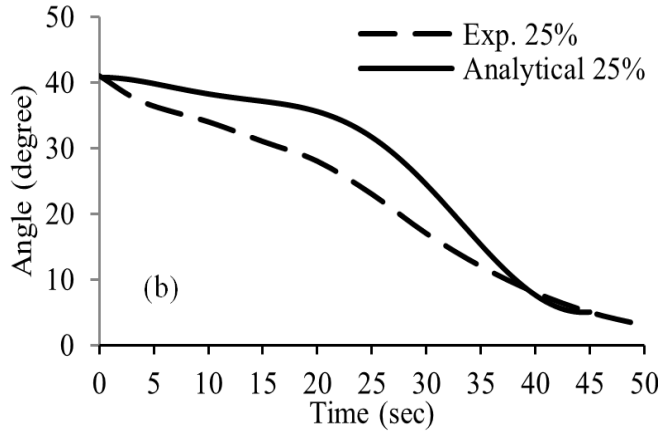

b)

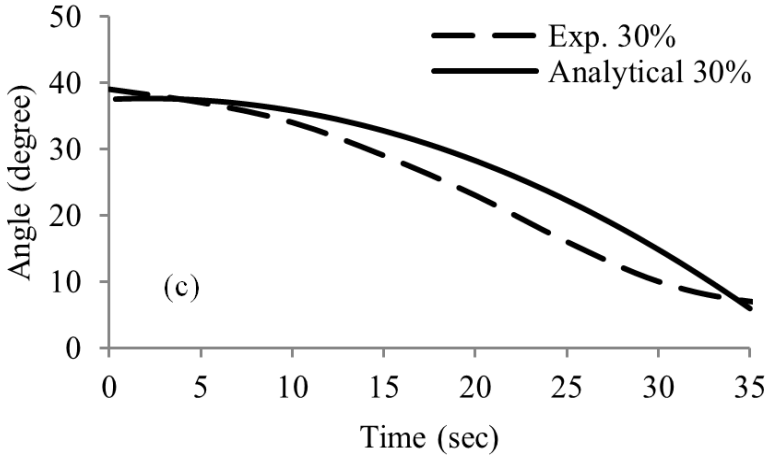

c)

Figure 11. Recovery angle-time relationship for (a) 20%, (b) 25% and (c) 30% SMPCs

5. Conclusion

The outcome of fibre reinforcement on the shape memory behavior of SMP has been analytically investigated in this paper. A mathematical model for the behavior of SMP material and its fiber composite is developed based on the stimulus temperature-time relation, and validated using experimental investigations.

- The model results showed excellent prediction ability for the shape recovery behavior with a slight deviation of (8%-16%) from the experimental results.
- The model findings showed significant reduction in recovery time of 25% and 41% when the fiber content increased from 20% to 25% and 30%, respectively.
- The experimental results revealed significant improvement in thermomechanical properties due to the fiber reinforcement, this includes 5oC increase in Tg and five orders increase in storage modulus.
- Also, the shape recovery rate is improved up to 80%, though a minor reduction in shape fixity of 7% was recognized.

Presented model represents a quick and easy tool kit for future studies that targeting the analysis of SMPCs shape recovery performance.

References

[1] M. Fejős and J. Karger-Kocsis, "Shape memory performance of asymmetrically reinforced epoxy/carbon fibre fabric composites in flexure," *Express Polym. Lett*, vol. 7, pp. 528-534, 2013.

[2] M. Staszczak, M. Nabavian Kalat, K. M. Golasiński, L. Urbański, K. Takeda, R. Matsui, and E. A. Pieczyska, "Characterization of polyurethane shape memory polymer and determination of shape fixity and shape recovery in subsequent thermomechanical cycles," *Polymers*, vol. 14, p. 4775, 2022.

[3] T. Ohki, Q.-Q. Ni, N. Ohsako, and M. Iwamoto, "Mechanical and shape memory behavior of composites with shape memory polymer," *Composites Part A: Applied Science and Manufacturing*, vol. 35, pp. 1065-1073, 9// 2004.

[4] H. Holman, M. N. Kavarana, and T. K. Rajab, "Smart materials in cardiovascular implants: Shape memory alloys and shape memory polymers," *Artificial Organs*, vol. 45, pp. 454-463, 2021.

[5] Z. Liu, Q. Li, W. Bian, X. Lan, Y. Liu, and J. Leng, "Preliminary test and analysis of an ultralight lenticular tube based on shape memory polymer composites," *Composite Structures*, vol. 223, p. 110936, 2019.

[6] E. R. Abrahamson, M. S. Lake, N. A. Munshi, and K. Gall, "Shape memory mechanics of an elastic memory composite resin," *Journal of Intelligent Material Systems and Structures*, vol. 14, pp. 623-632, 2003.

[7] W. Al Azzawi, J. A. Epaarachchi, M. Islam, and J. Leng, "Implementation of a finite element analysis procedure for structural analysis of shape memory behaviour of fibre reinforced shape memory polymer composites," *Smart Materials and Structures*, vol. 26, p. 125002, 2017.

[8] M. Fejős, G. Romhany, and J. Karger-Kocsis, "Shape memory characteristics of woven glass fibre fabric reinforced epoxy composite in flexure," *Journal of Reinforced Plastics and Composites*, p. 0731684412461541, 2012.

[9] J.-H. Roh, H.-J. Kim, and J.-S. Bae, "Shape memory polymer composites with woven fabric reinforcement for self-deployable booms," *Journal of Intelligent Material Systems and Structures*, p. 1045389X14544148, 2014.

[10] M. Kim, S. Jang, S. Choi, J. Yang, J. Kim, and D. Choi, "Analysis of shape memory behavior and mechanical properties of shape memory polymer composites using thermal conductive fillers," *Micromachines*, vol. 12, p. 1107, 2021.

[11] X. Lan, Y. Liu, H. Lv, X. Wang, J. Leng, and S. Du, "Fiber reinforced shape-memory polymer composite and its application in a deployable hinge," *Smart Materials and Structures*, vol. 18, p. 024002, 2009.

[12] Y. Li, J. Ye, L. Liu, B. Shi, and Y. He, "A Novel Microscopic Modeling Scheme for the Shape Memory Polymer Composites with respect to the Ambient Temperature," *International Journal of Aerospace Engineering*, vol. 2022, 2022.

[13] Y. Wang, H. Zhou, Z. Liu, X. Peng, and H. Zhou, "A 3D anisotropic visco-hyperelastic constitutive model for unidirectional continuous fiber reinforced shape memory composites," *Polymer Testing*, vol. 114, p. 107712, 2022.

[14] L. Bhola, A. K. Saurav, P. Mujumdar, and P. Guruprasad, "A numerical approach for modeling

response of shape memory polymer composite corrugated structure," *Smart Materials and Structures*, 2023.

[15] T. Yang, W. Chen, G. Fang, Z. Cao, B. Zhao, and X. Zhang, "Experiments and Simulations on the Shape Memory Process of Thermally-Induced Shape Memory Polymer Composite Thin-Wall Structure Considering Progressive Damage," *Applied Composite Materials*, pp. 1-25, 2023.

[16] F. Qin, F. Lu, K. Chen, Y. Hou, C. Zhang, and L. Huang, "Numerical simulation and experimental validation of ratchetting deformation of short fiber-reinforced polymer composites," *Composites Part B: Engineering*, vol. 266, p. 110974, 2023.

[17] S. Kiyani, F. Taheri-Behrooz, and A. Asadi, "Analytical and numerical study of shape memory polymers as intervertebral discs under pure bending," *Polymer Testing*, vol. 120, p. 107943, 2023.

[18] Y. Liu, K. Gall, M. L. Dunn, A. R. Greenberg, and J. Diani, "Thermomechanics of shape memory polymers: uniaxial experiments and constitutive modeling," *International Journal of Plasticity*, vol. 22, pp. 279-313, 2006.

[19] W. Al Azzawi, M. M. Islam, J. Leng, F. Li, and J. A. Epaarachchi, "Quantitative and qualitative analyses of mechanical behavior and dimensional stability of styrene-based shape memory composites," *Journal of Intelligent Material Systems and Structures*, vol. 28, pp. 3115-3126, 2017.

[20] M. Baghani and A. Taheri, "An analytic investigation on behavior of smart devices consisting of reinforced shape memory polymer beams," *Journal of Intelligent Material Systems and Structures*, vol. 26, pp. 1385-1394, 2015.

[21] Q. Tan, L. Liu, Y. Liu, and J. Leng, "Thermal mechanical constitutive model of fiber reinforced shape memory polymer composite: based on bridging model," *Composites Part A: Applied Science and Manufacturing*, vol. 64, pp. 132-138, 2014.

[22] M. Baghani, R. Naghdabadi, and J. Arghavani, "A large deformation framework for shape memory polymers: Constitutive modeling and finite element implementation," *Journal of Intelligent Material Systems and Structures*, September 5, 2012 2012.

[23] J.-H. Roh, H.-J. Kim, and J.-S. Bae, "Shape memory polymer composites with woven fabric reinforcement for self-deployable booms," *Journal of Intelligent Material Systems and Structures*, vol. 25, pp. 2256-2266, 2014.